PAPER Special Section on Recent Progress in Electromagnetic Theory and Its Application

Scattering of TM Plane Wave from Periodic Grating with Single Defect

Kazuhiro HATTORI[†a)], **Junichi NAKAYAMA**[†b)], *and* **Yasuhiko TAMURA**[†c)], *Members*

SUMMARY This paper deals with the scattering of a TM plane wave from a periodic grating with single defect, of which position is known. The surface is perfectly conductive and made up with a periodic array of rectangular grooves and a defect where a groove is not formed. The scattered wave above grooves is written as a variation from the diffracted wave for the perfectly periodic case. Then, an integral equation for the scattering amplitude is obtained, which is solved numerically by use of truncation and the iteration method. The differential scattering cross section and the optical theorem are calculated in terms of the scattering amplitude and are illustrated in figures. It is found that incoherent Wood's anomaly appears at critical angles of scattering. The physical mechanisms of Wood's anomaly and incoherent Wood's anomaly are discussed in relation to the guided surface wave excited by the incident plane wave. It is concluded that incoherent Wood's anomaly is caused by the diffraction of the guided surface wave.

key words: *scattering, periodic grating, defect, TM plane wave, rectangular grooves, incoherent Wood's anomaly, guided surface wave*

1. Introduction

In electronics, there are many devices which have periodic structure with rectangular parallel lines such as LCD electrodes. Defects in such periodic structure have been a serious problem for years. For developing an optical method of measurement and inspection, this paper studies a simple model, which is the wave scattering from a periodic array of rectangular grooves with single defect shown in Fig. 1.

Although there are many works [1]–[7] on the scattering and diffraction by a single groove, a finite number of grooves and an infinite periodic array of grooves without any defects, the scattering from a periodic grating with defects has not been studied extensively. However, we have studied the scattering of a TE plane wave from a periodic grating with single defect [8].

This paper deals with the TM case. The surface is perfectly conductive and made up with a periodic array of rectangular grooves and a defect at a known position, where a groove is not formed. We write the wave field above the grooves as a sum of the diffracted wave and the scattered wave as a variation from a perfectly periodic case. On the other hand, the field inside the grooves is expressed as a sum of guided modes with unknown mode amplitudes by use of the modal expansion method [9]. We derive an integral equation for the scattering amplitude from the boundary condition. Then, we numerically obtain the scattering amplitude by use of truncation and the iteration method starting from the diagonal approximation solution as an initial value. The differential scattering cross section and the optical theorem are calculated in terms of the scattering amplitude and are illustrated in figures.

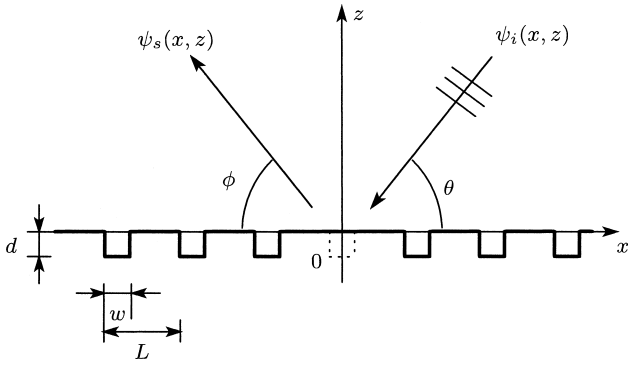

Fig. 1 Scattering of TM plane wave from a periodic grating with single defect. The surface is a periodic array of rectangular grooves and has a defect where a groove is not formed. $\psi_i(x,z)$ is the incident wave and $\psi_s(x,z)$ is the scattered wave. θ is the angle of incidence, ϕ is the scattering angle, L is the period of surface, w and d are the width and the depth of groove.

As is well known, in the perfectly periodic case, Wood's anomaly appears for critical angles of incidence as rapid variations of the diffraction powers. In the case of a periodic grating with defect, however, another anomaly, which we call incoherent Wood's anomaly, appears at critical angles of scattering as rapid variations in the angular distribution of the scattering. In this paper, we discuss the physical mechanisms of Wood's anomaly and incoherent Wood's anomaly. Incoherent Wood's anomaly has been found in cases of periodic random surfaces [10], [11]. However, we newly find that such anomaly appears in the case of a periodic surface with single defect.

The time dependence $e^{-i2\pi f_0 t}$ is assumed and suppressed throughout the paper.

2. Mathematical Formulation of the Problem

2.1 Periodic Grating with Single Defect

Let us consider a periodic array of rectangular grooves with single defect at $x = 0$ (See Fig. 1). We write such an array

Manuscript received April 18, 2007.
Manuscript revised July 17, 2007.

[†]The authors are with the Graduate School of Engineering and Design, Kyoto Institute of Technology, Kyoto-shi, 606-8585 Japan.
a) E-mail: kazuhirin@nifty.com
b) E-mail: nakayama@kit.ac.jp
c) E-mail: ytamura@kit.ac.jp

DOI: 10.1093/ietele/e91–c.1.17

as

$$z = f(x) = f_p(x) + d \cdot u(x|w), \tag{1}$$

$$f_p(x) = -d \sum_{g=-\infty}^{\infty} u(x-gL|w), \tag{2}$$

where L is the period, w and d are the width and the depth of a groove. $f_p(x)$ is a perfectly periodic surface without defect and the second term in (1) expresses the defect. Here, $u(x|w)$ is a rectangular groove defined as

$$u(x|w) = \begin{cases} 1, & |x| \le w/2, \\ 0, & |x| > w/2. \end{cases} \tag{3}$$

It has the orthogonal property such that

$$u(x-gL|w)u(x-g'L|w) = \delta_{gg'}u(x-gL|w), \quad (g, g' = 0, \pm1, \pm2, \cdots), \tag{4}$$

where $\delta_{gg'}$ is Kronecker's delta. For convenience, we put k_L and k_w as

$$k_w = \pi/w, \quad k_L = 2\pi/L, \tag{5}$$

and we define an auxiliary function $c_m(q)$ as follows.

$$c_m(q) = \int_{-\infty}^{\infty} u(x|w)\cos(mk_w(x+w/2))e^{-iqx}dx, \tag{6}$$

where m is integer. Note that $c_m(q) \sim 1/q$ when $|q|$ becomes large.

We denote the y component of the magnetic field by $\Psi(x, z)$, which satisfies the Helmholtz equation

$$\left[\frac{\partial^2}{\partial x^2} + \frac{\partial^2}{\partial z^2} + k^2\right]\Psi(x, z) = 0, \tag{7}$$

in the region $z > f(x)$. Here, $k = 2\pi/\lambda$ is wavenumber and λ is wavelength. On the surface $z = f(x)$, the wave field $\Psi(x, z)$ satisfies the Neumann condition,

$$\left.\frac{\partial\Psi(x, z)}{\partial n}\right|_{z=f(x)} = 0. \tag{8}$$

We write the incident plane wave $\psi_i(x, z)$ as

$$\psi_i(x, z) = e^{ipx}e^{-i\beta_0(p)z}, \quad p = -k\cos\theta, \tag{9}$$

$$\beta_n(p) = \beta_0(p+nk_L) = \sqrt{k^2-(p+nk_L)^2}, \tag{10}$$

$$Im[\beta_n(p)] \ge 0, \quad (n = 0, \pm1, \pm2, \cdots), \tag{11}$$

where θ is the angle of incidence (See Fig. 1) and Im stands for the imaginary part.

2.2 Diffraction by a Perfectly Periodic Grating

First, we consider a perfectly periodic case. For the region $z \ge 0$, we write the y component of the magnetic field $\hat{\Psi}_1(x, z)$ as a sum of the incident wave $\psi_i(x, z)$ and the diffracted wave $\psi_d(x, z)$ due to the periodicity of the surface,

$$\hat{\Psi}_1(x, z) = e^{ipx}e^{-i\beta_0(p)z} + \psi_d(x, z), \tag{12}$$

$$\psi_d(x, z) = e^{ipx}\sum_{n=-\infty}^{\infty} A_n(p)e^{ink_Lx+i\beta_n(p)z}. \tag{13}$$

Here, $A_n(p)$ is the amplitude of the nth order Floquet mode. On the other hand, by use of the modal expansion method [9], we write the y component of the magnetic field inside the grooves $\hat{\Psi}_2(x, z)$ as a sum of the guided modes,

$$\hat{\Psi}_2(x, z) = \sum_{g=-\infty}^{\infty} u(x-gL|w)e^{ipgL}\sum_{m=0}^{\infty} Q_m^c(p) \times\cos(mk_w(x+w/2-gL))\cos(\gamma_m(z+d)), \tag{14}$$

$$\gamma_m = \sqrt{k^2-(mk_w)^2}, \tag{15}$$

where $Q_m^c(p)$ is the amplitude of the guided mode which we call the base component, and γ_m is the propagation constant of the mth guided mode. Note that the guided mode number starts from $m = 0$ in the TM case.

The energy conservation relation for the perfectly periodic case can be obtained [8] as

$$1 = \sum_{n=-\infty}^{\infty} Re[\beta_n(p)]|A_n(p)|^2/\beta_0(p). \tag{16}$$

Here, Re denotes the real part and $Re[\beta_n(p)]|A_n(p)|^2/\beta_0(p)$ is the nth order relative diffraction power, which will be illustrated below.

2.3 Solution for a Perfectly Periodic Grating

Let us determine $A_n(p)$ and $Q_m^c(p)$ from the continuity of both the magnetic field and the electric field at $z = 0$.

We start with a boundary condition $[\partial\hat{\Psi}_1/\partial z - \partial\hat{\Psi}_2/\partial z]_{z=0} = 0$. Multiplying this by $e^{-i(p+nk_L)x}$ and integrating over one period L, we get

$$i\beta_n(p)LA_n(p) - i\beta_0(p)L\delta_{n0} = -\sum_{m=0}^{\infty}\gamma_m Q_m^c(p)\sin(\gamma_m d)c_m(p+nk_L). \tag{17}$$

Next, we have another boundary condition $\sum_{g=-\infty}^{\infty} u(x-gL|w)[\hat{\Psi}_1(x, 0) - \hat{\Psi}_2(x, 0)] = 0$. Taking Fourier transform of this after multiplying $u(x-gL|w)\times\cos(mk_w(x+w/2-gL))$, we obtain

$$\sum_{n=-\infty}^{\infty} A_n(p)c_m(-p-nk_L) + c_m(-p) = \frac{wQ_m^c(p)}{2}\cos(\gamma_m d)(1+\delta_{m0}). \tag{18}$$

Here, (17) and (18) are infinitely dimensional equations. By use of truncation [9], [12], we will numerically solve (17) and (18) to obtain $A_n(p)$ and $Q_m^c(p)$.

In what follows, we always consider a non-resonance case, that is, $\cos(\gamma_m d) \ne 0$ for any m. Eliminating $Q_m^c(p)$ from (17) and (18), we get an equation for $A_n(p)$ as

$$\sum_{l=-\infty}^{\infty}[i\beta_n(p)\delta_{nl} + k_L M(p+nk_L, p+lk_L)]A_l(p)$$

$$= i\beta_0(p)\delta_{n0} - k_L M(p+nk_L, p), \tag{19}$$

where k_L is defined in (5), $i\beta_0(p)\delta_{n0}$ is an excitation by the incident wave and $M(s, s')$ is a coupling factor defined as

$$M(s, s') = \sum_{m=0}^{\infty} \frac{\gamma_m \tan(\gamma_m d)}{\pi w(1+\delta_{m0})} c_m(s) c_m(-s'), \tag{20}$$

where the difference $s - s'$ works as a Bragg vector. When the depth of the grooves d is small, $M(s, s')$ becomes small. We regard (19) as an infinitely dimensional matrix equation for $A_n(p)$. Thus, the inverse matrix of $[i\beta_n(p)\delta_{nl} + k_L M(p + nk_L, p + lk_L)]$ can be considered as Green's function of the periodic grating in the spectral domain. Since the periodic surface $f_p(x)$ has a discrete spectrum, $M(p + nk_L, p + lk_L)$ represents the discrete Bragg coupling from $A_l(p)$ to $A_n(p)$, where $(p+nk_l)-(p+lk_L) = (n-l)k_L$ is the Bragg vector transforming the wave vector $p + lk_L$ of $A_l(p)$ to $p + nk_L$ of $A_n(p)$. When $p = -k\cos\theta \approx \pm k + lk_L$ ($l = \pm 1, \pm 2, \cdots$) holds, i.e., $\theta \approx \cos^{-1}(\mp 1 - lk_L/k)$, a well-known phenomenon, so-called Wood's anomaly [12], [13], occurs as a rapid variation of the diffraction amplitude. However, as far as the authors know, there have been few discussions on the physical mechanism of Wood's anomaly in the periodic cases. We will point out that such an anomaly is caused by a coupling with guided surface waves [11] in what follows.

In the single defect case, however, the surface $f(x)$ has a continuous component in the spectrum. Thus, a continuous Bragg coupling appears in the case with defect, as is discussed below.

2.4 Scattering from a Periodic Grating with Single Defect

The single defect in a periodic grating generates the scattering. We express such scattering as a variation from the diffracted wave for the perfectly periodic case. Thus, we write for $z > 0$,

$$\Psi_1(x, z) = \hat{\Psi}_1(x, z) + \psi_s(x, z), \tag{21}$$

$$\psi_s(x, z) = e^{ipx} \int_{-\infty}^{\infty} a(s|p) e^{isx + i\beta_0(p+s)z} ds, \tag{22}$$

where $\psi_s(x, z)$ is the scattered wave due to the defect and $a(s|p)$ is the scattering amplitude. Since $\psi_s(x, z)$ is scattered from the single defect, we assume that $\psi_s(x, z)$ satisfies Sommerfeld's radiation condition, that is, $\psi_s(r\cos\theta, r\sin\theta) \sim f(\theta)e^{ikr}/\sqrt{kr}$ ($r = \sqrt{x^2 + z^2}$) and is expected to decay at $kr \to \infty$.

On the other hand, we write the wave field inside the grooves $\Psi_2(x, z)$ as a sum of the wave field for the perfectly periodic grating and the fluctuated term $\psi_G(x, z)$ due to the defect.

$$\Psi_2(x, z) = \hat{\Psi}_2(x, z) + \psi_G(x, z),$$

$$\psi_G(x, z) = \sum_{g=-\infty}^{\infty} u(x - gL|w) e^{ipgL} \sum_{m=0}^{\infty} q_m^{(g)}(p) \times \cos(mk_w(x + w/2 - gL)) \cos(\gamma_m(z + d))$$

$$- u(x|w) \sum_{m=0}^{\infty} Q_m^c(p) \times \cos(mk_u(x + w/2)) \cos(\gamma_m(z + d)). \tag{23}$$

Here, $q_m^{(g)}(p)$ is the perturbed amplitude of the mth guided mode in the gth groove. Note that $q_m^{(0)}(p) \equiv 0$ for all m since a groove is not formed at $g = 0$.

2.5 Optical Theorem and Scattering Cross Section

The optical theorem for the single defect case can be obtained from the identity $Im[\mathrm{div}\Psi_1 \mathrm{grad}\Psi_1^*] = 0$ as [8]

$$P_c = \Phi_s, \tag{24}$$

$$P_c = -\frac{2}{k} \sum_{n=-\infty}^{\infty} Re[\beta_n^*(p)] Re[a(k_L n|p) A_n^*(p)], \tag{25}$$

$$\Phi_s = \frac{1}{k} \int_{-\infty}^{\infty} Re[\beta_0(p+s)] |a(s|p)|^2 ds = \frac{L}{2\pi} \int_0^{\pi} \sigma(\phi|\theta) d\phi, \tag{26}$$

which is an extension of the forward scattering theorem [14], [15]. Here, the asterisk denotes the complex conjugate, P_c is related to the reduction of the scattering amplitude, Φ_s expresses the total scattering cross section and $\sigma(\phi|\theta)$ is the differential scattering cross section per period

$$\sigma(\phi|\theta) = \frac{2\pi k \sin^2\phi\, |a(-k\cos\phi - p|p)|^2}{L}, \tag{27}$$

where $\phi = \cos^{-1}(-(p + s)/k)$ is a scattering angle (See Fig. 1). Note that $\sigma(\phi|\theta)$ has no dimension. The optical theorem (24) can be used to estimate accuracy of a numerical solution.

2.6 Scattered Wave Field by Single Defect

Let us obtain equations for $a(s|p)$ and $q_m^{(g)}(p)$ from the continuity of both the magnetic field and the electric field. From $[\partial\Psi_1/\partial z - \partial\Psi_2/\partial z]|_{z=0} = 0$, we have $[\partial\psi_s/\partial z - \partial\psi_G/\partial z]|_{z=0} = 0$. Taking Fourier transform of this relation and multiplying $e^{-i(p+s)x}/2\pi$, we obtain an equation for $a(s|p)$ and $q_m^{(g)}(p)$ as

$$i\beta_0(p+s)a(s|p) = \frac{1}{2\pi} \sum_{m=0}^{\infty} \gamma_m c_m(p+s) \sin(\gamma_m d) \times \left[Q_m^c(p) - \sum_{g=-\infty}^{\infty} e^{-isgL} q_m^{(g)}(p) \right]. \tag{28}$$

On the other hand, from $\sum_{g\neq 0} u(x - gL|w)[\Psi_1(x, 0) - \Psi_2(x, 0)] = 0$, we obtain $\sum_{g\neq 0} u(x - gL|w)[\psi_s(x, 0) - \psi_G(x, 0)] = 0$. Then, taking Fourier transform of this after multiplying $u(x - gL|w) \times \cos(mk_w(x + w/2 - gL))$, we obtain

$$\left(1 - \delta_{g0}\right) \int_{-\infty}^{\infty} c_m(-p-s) e^{isgL} a(s|p) ds = \frac{w}{2} q_m^{(g)}(p) \cos(\gamma_m d)(1 + \delta_{m0}). \tag{29}$$

Here, (28) and (29) are infinitely dimensional. However,

these equations can be solved approximately by use of truncation.

Substituting (29) into (28), we get

$$i\beta_0(p+s)a(s|p)=\frac{1}{2\pi}\sum_{m=0}^{\infty}\gamma_m c_m(p+s)\sin(\gamma_m d)\times\left(Q_m^c(p)-\sum_{g=-\infty}^{\infty}e^{-isgL}\frac{1-\delta_{g0}}{\frac{w}{2}\cos(\gamma_m d)(1+\delta_{m0})}\times\int_{-\infty}^{\infty}c_m(-p-s')e^{is'gL}a(s|p)ds'\right). \quad (30)$$

Taking the sum on g and using the Fourier series representation of delta pulse series

$$\sum_{g=-\infty}^{\infty}e^{isgL}=k_L\sum_{l=-\infty}^{\infty}\delta(s-lk_L), \quad (31)$$

then we get an integral equation for the scattering amplitude $a(s|p)$ as

$$\sum_{l=-\infty}^{\infty}[i\beta_0(p+s)\delta_{l0}+k_L M(p+s,p+s+lk_L)]a(s+lk_L|p)=\sum_{m=0}^{\infty}\frac{\gamma_m}{2\pi}c_m(p+s)\sin(\gamma_m d)Q_m^c(p)+\int_{-\infty}^{\infty}M(p+s,p+s')a(s'|p)ds', \quad (32)$$

which is analogous in form with (19). Here, $M(p+s, p+s+lk_L)$ on the left-hand side represents a discrete Bragg coupling due to the surface periodicity, whereas $M(p+s, p+s')$ on the right-hand side is a continuous coupling due to the single defect.

We regard (32) as an infinitely dimensional matrix equation for $a(s|p)$. Thus, the inverse matrix of $[i\beta_0(p+s)\delta_{l0}+k_L M(p+s,p+s+lk_L)]$ may be considered as Green's function of the periodic grating with single defect. When $p+s=-k\cos\phi\approx\pm k+lk_L$ $(l=\pm1,\pm2,\cdots)$ holds, the amplitude of the scattered wave into the direction $\phi\approx\cos^{-1}(\mp1-lk_L/k)$ changes rapidly as a function of the scattering angle ϕ, which we call incoherent Wood's anomaly. Such an anomaly may occur due to a strong coupling of the scattered wave with guided surface waves. We will discuss the physical mechanism of incoherent Wood's anomaly and show numerical examples of the anomaly in the angular distribution of the scattering below.

In what follows, we solve (32) by iteration.

2.7 Wood's Anomaly and Incoherent Wood's Anomaly

When $\beta_n(p)$ in (19) vanishes, the diffraction amplitude $A_n(p)$ may become large in a shallow case with $d\ll\lambda$. As is well known, this causes Wood's anomaly, which appears at critical angles of incidence as rapid variations of the diffraction powers against the angle of incidence.

First, we point out a mathematical fact. In a flat surface case without any roughness, TM plane waves $H_y=e^{\pm ikx\pm i\beta_0(\pm k)z}=e^{\pm ikx}$ are exact solutions of the Helmholtz Eq. (7) and satisfy the Neumann boundary condition $\partial H_y/\partial z=0$ at $z=0$ (See Fig. 2(a)). Therefore, a plane wave with the Rayleigh wavenumber $+k$ or $-k$ is a free guided wave propagating along the flat surface [16], [17]. Such a free guided wave does not exist in the TE case. When the surface has a periodic structure, such a free guided wave is scattered by the surface roughness and decays exponentially with propagation distance. As a result, it becomes a guided surface wave with a complex propagation constant $+s_p$ or $-s_p$ into the x direction (See Fig. 2(b)). Mathematically, such $\pm s_p$ are given as complex roots of the determinant of $[i\beta_n(p)\delta_{nl}+k_L M(p+nk_L,p+lk_L)]$. When the surface roughness is sufficiently small, however, we may expect that the complex propagation constant s_p exists very close to the Rayleigh wavenumber k[†]. In the case of a perfectly periodic surface, the surface has a discrete spectrum, and such a guided surface wave is excited by the incident wave due to the discrete Bragg coupling. Therefore, such excitation takes place only for the critical angles of incidence $\theta_W^{[l]}$, which are determined by

$$k^2-(-k\cos\theta_W^{[l]}-lk_L)^2=0,\quad (l=\pm1,\pm2,\cdots). \quad (33)$$

When the angle of incidence θ is critical, such a guided surface wave is excited and may have a large amplitude. Then, it is scattered by the periodic surface again. Thus, the multiple scattering takes place for a critical angle of incidence, which causes Wood's anomaly. As a result, Wood's anomaly appears as rapid variations of the diffraction powers. Note that, at $\theta=\theta_W^{[l]}$, the lth order Floquet mode becomes cutoff.

In the case of a periodic grating with single defect, another anomaly, which we call incoherent Wood's anomaly,

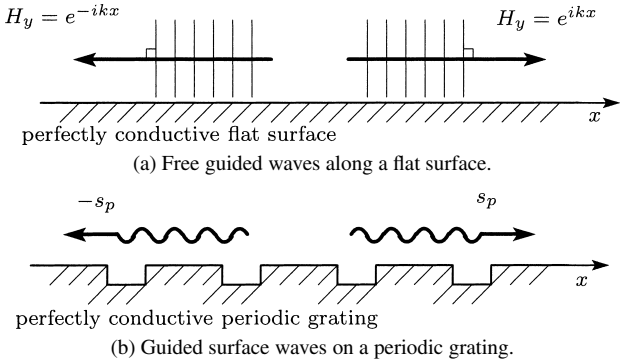

(a) Free guided waves along a flat surface.

(b) Guided surface waves on a periodic grating.

Fig. 2 (a) Free guided waves propagating into the x direction along a perfectly conductive flat surface without any roughness. Such free guided waves have the Rayleigh wavenumber $+k$ and $-k$, and satisfy the Helmholtz Eq. (7) and the Neumann boundary condition $\partial H_y/\partial z=0$ at $z=0$. (b) Guided surface waves propagating along the perfectly conductive grating. Guided surface waves have complex propagation constants $\pm s_p$ into the x direction.

[†]Since this complex propagation constant s_p should exist very close to the Rayleigh wavenumber k in the shallow case, we assume $Re(s_p)\approx k$ and put such complex s_p as real k in the following discussion for simplicity.

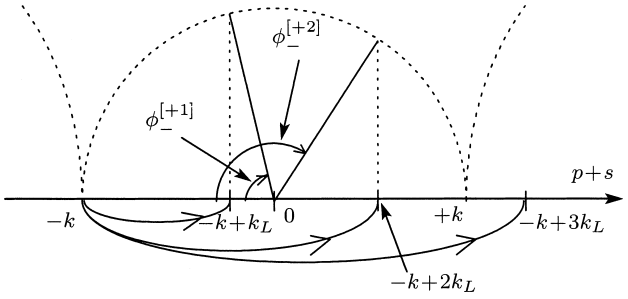

(a) Diffraction of the guided surface wave with the wavenumber near $-k$.

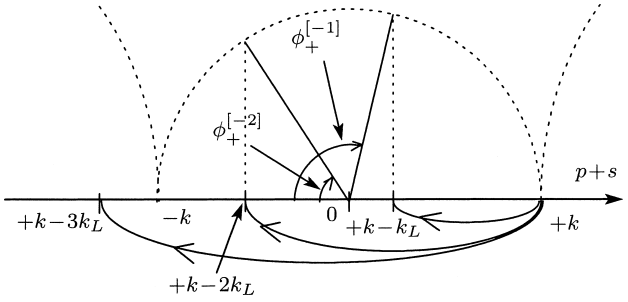

(b) Diffraction of the guided surface wave with the wavenumber near $+k$.

Fig. 3 Incoherent Wood's anomaly at critical angles of scattering (a) $\phi_-^{[+1]}$ and $\phi_-^{[+2]}$ and (b) $\phi_+^{[-1]}$ and $\phi_+^{[-2]}$ for $L = 1.3\lambda$.
(a) Guided surface wave with the wavenumber near $-k$ is diffracted into $-k+k_L$ and $-k+2k_L$ by the periodic grating. It is also diffracted to $-k+3k_L$ in the evanescent region. (b) Guided surface wave with the wavenumber near $+k$ is diffracted into $+k-k_L$ and $+k-2k_L$ by the periodic grating. It is also diffracted to $+k-3k_L$ in the evanescent region.

appears at several angles of scattering as rapid variations in the angular distribution of the scattering. The surface spectrum has a discrete component due to the periodicity and a continuous component due to the defect. Because of the scattering by the continuous component, such a guided surface wave is always excited by the incident plane wave with any angle of incidence and then diffracted into discrete directions by the discrete component. To describe these processes, we introduce a critical wavenumber $s_\pm^{[l]}$ as

$$s_\pm^{[l]} = \pm k - p + lk_L, \qquad (l = 0, \pm 1, \pm 2, \cdots). \tag{34}$$

Let us consider the solution $a(s|p)$ of (32). When $\beta_0(p+s) = 0$ and $s = s_\pm^{[0]} = \pm k - p$, the solution $a(s|p) = a(s_\pm^{[0]}|p)$ has a large amplitude, because $M(p+s, p+s+lk_L)$ is small in the shallow case. We regard $a(s_\pm^{[0]}|p)$ as the amplitude of the guided surface wave, which is diffracted into discrete directions. This means that $a(s_\pm^{[l]}|p) = a(\pm k - p + lk_L|p)$ could have a large amplitude for any integer l, due to the discrete Bragg coupling from $s_\pm^{[0]} = (\pm k - p)$ to $s_\pm^{[l]} = (\pm k - p + lk_L)$. Thus, we may observe incoherent Wood's anomaly at a critical angle of scattering $\phi_\pm^{[l]}$ (See Fig. 3),

$$p + s_\pm^{[l]} = \pm k + lk_L = -k\cos\phi_\pm^{[l]}, \tag{35}$$

$$\phi_\pm^{[l]} = \cos^{-1}\left(\mp 1 - l\frac{\lambda}{L}\right), \qquad (l = \pm 1, \pm 2, \cdots), \tag{36}$$

where the signs $\pm$ and $\mp$ go together in (36). In the numerical results below, we will see that $|a(s|p)|$ has a steep peak or dip at $s = s_\pm^{[l]} = \pm k + lk_L$. Note that $s_\pm^{[l]}$ and $\phi_\pm^{[l]}$ only depend on the period L and the wavelength λ and are independent of the angle of incidence θ.

Incoherent Wood's anomaly has been found in cases of periodic random surfaces [10], [11]. However, we newly show that it takes place in such a deterministic case as a periodic surface with single defect. We also note that incoherent Wood's anomaly appears in the TM case but does not occur in the TE case [8].

3. Numerical Examples

3.1 Perfectly Periodic Case

Here, we obtain some numerical examples for the perfectly periodic case. We determine the diffraction amplitude $A_n(p)$ and the base component $Q_m^c(p)$ by introducing the truncation numbers N_d and N_m. N_d is the truncation number of the diffraction orders and N_m is that of the guided modes inside the groove in the summation (17) and (18), which means that we assume

$$\begin{aligned} A_n(p) &= 0, \quad |n| > N_d, \\ Q_m^c(p) &= 0, \quad m > N_m. \end{aligned} \tag{37}$$

In this paper, we set

$$N_d = 10, \quad N_m = 20. \tag{38}$$

Thus, $[A_n(p)]$ becomes a $(2N_d+1)$-vector, $[Q_m^c(p)]$ becomes an (N_m+1)-vector in the calculation below.

Figure 4 illustrates the relative diffraction power against the angle of incidence θ for the periods $L = 1.3\lambda$ (upper figure) and $L = 1.7\lambda$ (lower figure) with the width $w = 0.7\lambda$ and the depth $d = 0.1\lambda$. The incident power is normalized to 1. The line '(0)' means the relative power of the 0th order Floquet mode, i.e, $Re[\beta_0(p)]|A_0|^2/\beta_0(p)$, and the line '(1)' that of the 1st order Floquet mode, and so on. Since the energy error is always less than 10^{-10}, the truncation numbers N_d and N_m in (38) are sufficient for the perfectly periodic case. For $L = 1.3\lambda$, the diffraction power changes rapidly near the critical angles $\theta_W^{[-2]} = 57.42°$ and $\theta_W^{[1]} = 76.66°$ given by (33). For $L = 1.7\lambda$, Wood's anomaly appears at critical angles $\theta_W^{[-3]} = 40.12°$, $\theta_W^{[1]} = 65.68°$ and $\theta_W^{[-2]} = 79.84°$.

3.2 Single Defect Case

Let us solve the integral Eq. (32) to obtain numerical examples for the single defect case. Here, we only consider the case with $w = 0.7\lambda$.

Since (32) is an equation for infinitely many unknowns and has an integral term including $a(s'|p)$, it is still an open question how to solve (32). In this paper, we attempt to solve (32) approximately by the iteration method. However, we introduce a single scattering approximation and a diagonal approximation.

First, neglecting $M(p+s, p+s+lk_L)$ and the integral term in (32), we obtain a single scattering solution $a^S(s|p)$

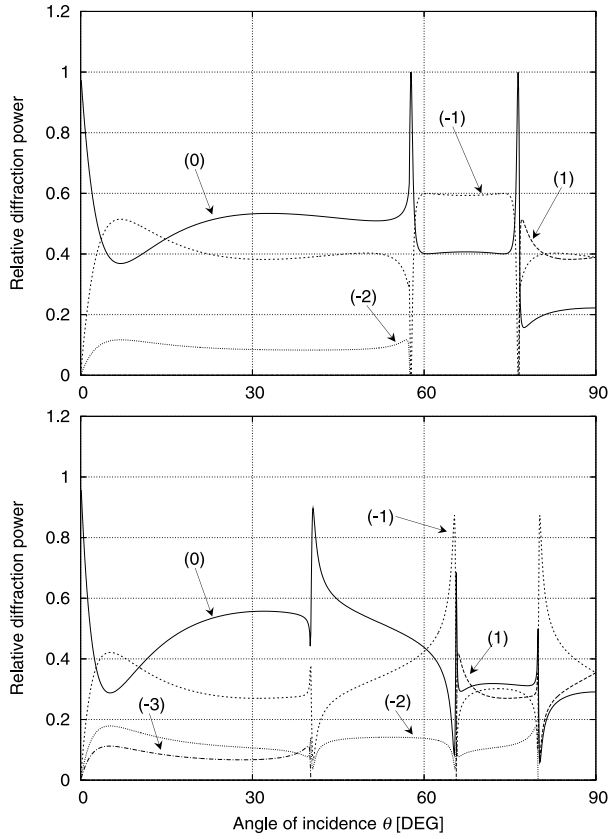

Fig. 4 Relative diffraction power against the angle of incidence θ for periods $L = 1.3\lambda$(upper figure), 1.7λ(lower figure) with depth $d = 0.1\lambda$ and width $w = 0.7\lambda$. Wood's anomaly occurs at angles where one particular diffraction mode disappears.

as

$$a^S(s|p) = \frac{1}{2\pi}\sum_{m=0}^{N_m}\frac{\gamma_m c_m(p+s)\sin(\gamma_m d)Q_m^c(p)}{i\beta_0(p+s)}, \tag{39}$$

where $\sum_{m=0}^{N_m}\gamma_m c_m(p+s)\sin(\gamma_m d)Q_m^c(p)$ represents the effect of the single defect, however, the discrete Bragg coupling and the continuous Bragg coupling are neglected. Since the factor $1/\beta_0(p+s)$ is the free space Green's function in the spectral domain, (39) does not involve effects of the scattering by the periodic surface.

Next, neglecting the integral term in (32), we obtain an equation for the diagonal approximation $a^D(s|p)$ with the truncation numbers N_l and N_m as

$$\sum_{l=-N_l}^{N_l}[i\beta_0(p+s)\delta_{l0}+k_L M(p+s, p+s+lk_L)]a^D(s+lk_L|p) = \sum_{m=0}^{N_m}\frac{\gamma_m}{2\pi}c_m(p+s)\sin(\gamma_m d)Q_m^c(p), \tag{40}$$

which is solved numerically. Such the diagonal approximation is analogous to the Gaussian random rough case discussed in [18]. The diagonal approximation $a^D(s|p)$ is then used as an initial guess of the iterative solution below.

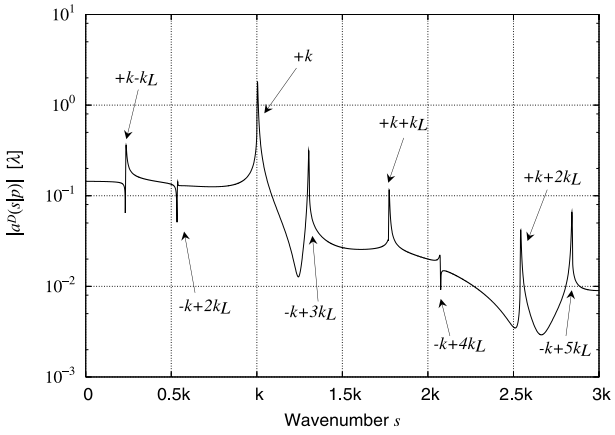

Fig. 5 Diagonal approximation $a^D(s|p)$ with $L = 1.3\lambda$, $d = 0.1\lambda$, $w = 0.7\lambda$ and $\theta = 90°$ ($p = 0$). $a^D(s|p)$ has steep peaks and dips at $s \approx +k$ and $s \approx s_\pm^{[l]} = \pm k + lk_L$ ($l = \pm1, \pm2, \cdots$).

To solve (32), however, we rewrite (32) as an iterative form,

$$\sum_{l=-N_l}^{N_l}[i\beta_0(p+s)\delta_{l0}+k_L M(p+s, p+s+lk_L)]a^{(N)}(s+lk_L|p) = \sum_{m=0}^{N_m}\frac{\gamma_m}{2\pi}c_m(p+s)\sin(\gamma_m d)Q_m^c(p) + \int_{-\xi-p}^{\xi-p}M(p+s, p+s')a^{(N-1)}(s'|p)ds', \tag{41}$$

where $^{(N)}$ is the iteration number and ξ is the truncated bandwidth of $a(s|p)$. We set the initial value as $a^{(0)}(s|p) = a^D(s|p)$ and iteration is repeated until $N = N_{ite}$. In this paper, we set N_l, N_{ite} and ξ as

$$N_l = 11, \quad N_{ite} = 21, \quad \xi = 3k. \tag{42}$$

Figure 5 illustrates the diagonal approximation $a^D(s|p)$ against wavenumber s with $L = 1.3\lambda$, $d = 0.1\lambda$, $\theta = 90°$ ($p = -k\cos\theta = 0$). As is discussed above, $a^D(s|p)$ becomes large at $s \approx -p + k = +k$, which means the guided surface wave propagating along the surface has a large amplitude at the Rayleigh wavenumber $\beta_0(p+s) = 0$. Such the guided surface wave is diffracted by the periodic surface. As a result, $a^D(s|p)$ has several steep peaks and dips at $s \approx s_\pm^{[l]} = \pm k + lk_L$ ($l = \pm1, \pm2, \cdots$) given by (35), and incoherent Wood's anomaly appears in the differential cross section at $\phi \approx \phi_\pm^{[l]}$.

Figure 6 illustrates the differential scattering cross section $\sigma(\phi|\theta)$ with $L = 1.3\lambda$, $d = 0.1\lambda$ and $\theta = 60°$. Here, the iterative solution by (41) is compared with the single scattering solution (39). We see that, in the differential scattering cross section $\sigma(\phi|\theta)$ by the iterative solution, incoherent Wood's anomaly appears near the critical angles of scattering, which are calculated by (36) with $L = 1.3\lambda$ as $\phi_+^{[-2]} = 57.42°$, $\phi_-^{[1]} = 76.66°$, $\phi_+^{[-1]} = 103.34°$ and $\phi_-^{[2]} = 122.58°$. It is important to note that the iterative solution $a^{(N)}(s|p)$ gives $\sigma(\pi|\theta) = 0$ and $\sigma(0|\theta) = 0$, which mean

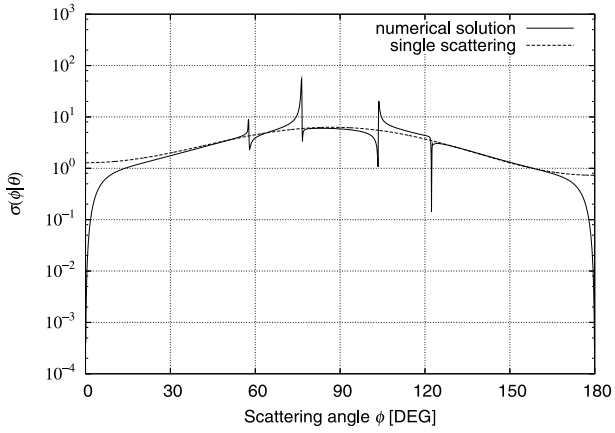

Fig. 6 Comparison of differential scattering cross section $\sigma(\phi|\theta)$ by numerical solution and single scattering approximation with $L = 1.3\lambda$, $d = 0.1\lambda$ and $w = 0.7\lambda$ and $\theta = 60°$.

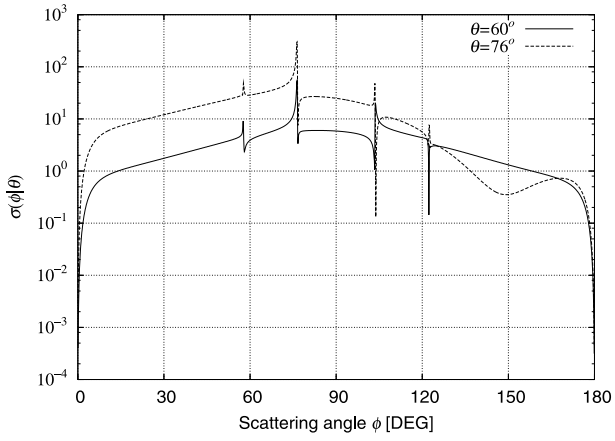

Fig. 7 Differential scattering cross section $\sigma(\phi|\theta)$ for $\theta = 60°$ and 76° with $L = 1.3\lambda$, $d = 0.1\lambda$ and $w = 0.7\lambda$.

that no scattering takes place into grazing directions due to the periodic surface. On the other hand, the single scattering approximation $a^S(s|p)$ yields no peaks and dips in the differential scattering cross section $\sigma(\phi|\theta)$. But it gives non-vanishing amplitudes for $\sigma(\pi|\theta)$ and $\sigma(0|\theta)$. This is because the single scattering approximation neglects the scattering by the periodic surface. In the following calculation, the iterative solution $a^{(N)}(s|p)$ is used to evaluate $\sigma(\phi|\theta)$.

Figure 7 illustrates $\sigma(\phi|\theta)$ for $\theta = 76°$ and 60° with $L = 1.3\lambda$ and $d = 0.1\lambda$. This figure shows that the critical scattering angles at which incoherent Wood's anomaly appears are independent of the incident angles θ. For $\theta = 76°$, however, the total scattering cross section becomes much larger than that with $\theta = 60°$. This is because $\theta = 76°$ is close to a critical angle of incidence $\theta_W^{[1]} = 76.66°$. This point will be shown later.

Figure 8 illustrates $\sigma(\phi|\theta)$ for $L = 1.3\lambda$ and $L = 1.7\lambda$ with $d = 0.1\lambda$ and $\theta = 60°$. It can be seen that scattering angles at which incoherent Wood's anomaly appears depend on the period L and the wavelength λ. This is because $\phi_\pm^{[l]}$ is dependent on the period. Figure 9 illustrates $\sigma(\phi|\theta)$ for $d = 0.1\lambda$ and $d = 0.05\lambda$ with $L = 1.3\lambda$ and $\theta = 60°$. Behavior of $\sigma(\phi|\theta)$ near $\phi_+^{[-2]}$ and $\phi_-^{[1]}$ is shown in the lower figure. It is found that, in the shallow case with $d = 0.05\lambda$, anomalous peaks and dips become narrow and steep.

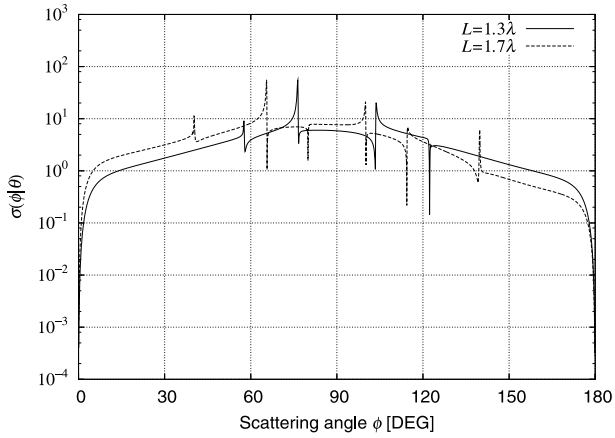

Fig. 8 Differential scattering cross section $\sigma(\phi|\theta)$ for $L = 1.3\lambda$ and 1.7λ with $w = 0.7\lambda$, $d = 0.1\lambda$ and $\theta = 60°$.

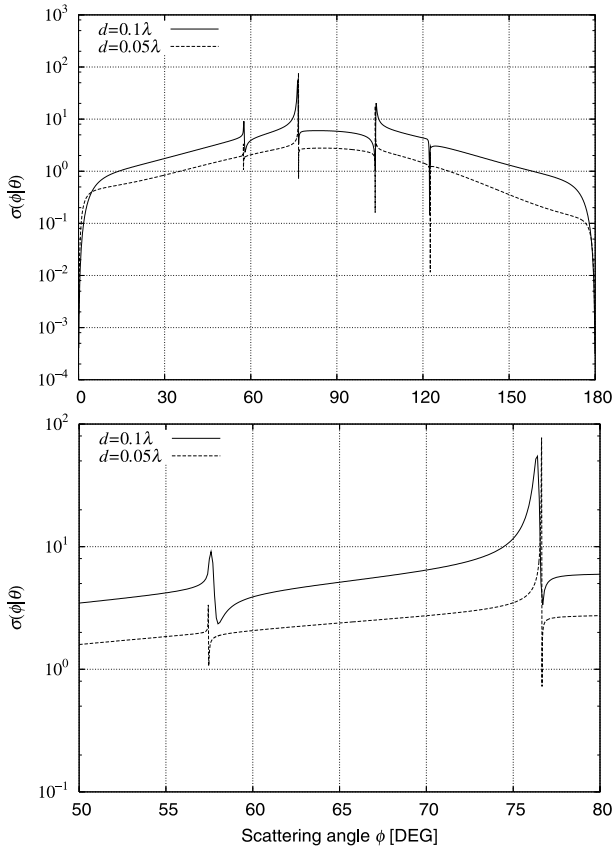

Fig. 9 Differential scattering cross section $\sigma(\phi|\theta)$ for $d = 0.1\lambda$ and $d = 0.05\lambda$ with $L = 1.3\lambda$, and $\theta = 60°$(upper figure), and the behavior of $\sigma(\phi|\theta)$ near $\phi_W^{[l]}$ (lower figure). Widths of the peaks and dips are smaller for $d = 0.05\lambda$.

Figure 10 illustrates the total scattering cross section Φ_s and the reduction of the scattering amplitude P_c against θ for $L = 1.3\lambda$, $d = 0.1\lambda$ in the upper figure. The total

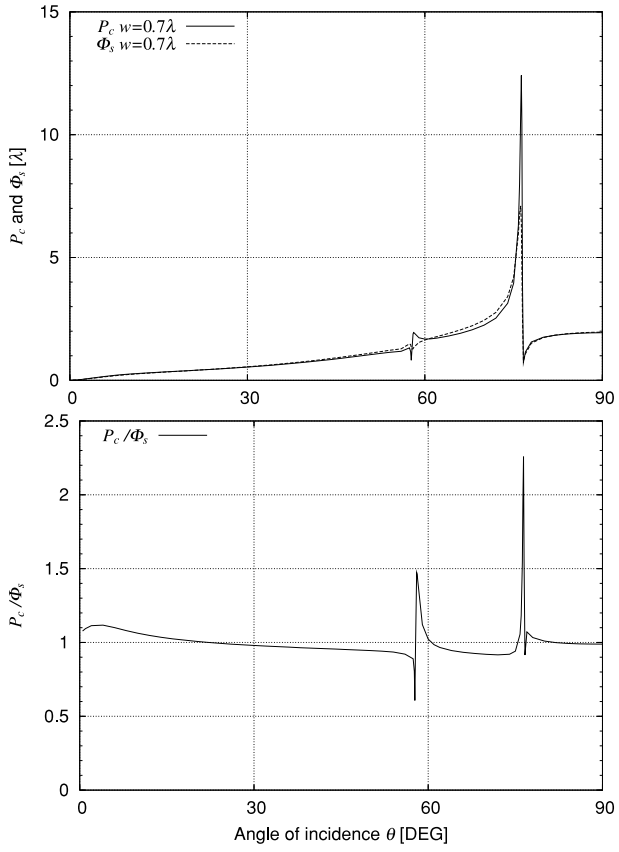

Fig. 10 Optical theorem against θ for $w = 0.7\lambda$ with $L = 1.3\lambda$, $d = 0.1\lambda$. P_c and Φ_s are shown in the upper figure, while the normalized optical theorem P_c/Φ_s is shown in the lower figure.

scattering cross section Φ_s is drawn with dots, while the reduction of scattering amplitude P_c is shown with line. The normalized optical theorem P_c/Φ_s is shown in the lower figure. However, P_c and Φ_s becomes large when the angle of incidence θ is close to one of the critical angles of incidence $\theta_W^{[1]} = 76.66°$. From the lower figure of Fig. 10, it is found that error $|1 - P_c/\Phi_s|$ is less than 0.1 for any angles of incidence except for ones close to the critical angle of incidence $\theta_W^{[l]}$ and grazing angle incidence smaller than 10°. For the incident angles close to $\theta_W^{[l]}$, error become large, which suggests that the iterative solution of the integral equation has limitation to apply and other approaches might be necessary to obtain a highly accurate solution.

4. Conclusions

We have considered the scattering of a TM plane wave from a periodic grating with single defect. We wrote the scattered wave above the grooves as a variation from the diffracted wave for the perfectly periodic case. Then, we obtained an integral equation for the scattering amplitude, which is solved by the iteration method using the diagonal approximation solution as an initial guess.

We found that incoherent Wood's anomaly appears in the differential scattering cross section for the periodic grating with single defect. The critical angles of scattering where incoherent Wood's anomaly appears only depend on the period of the grating and the wavelength, and are independent of the angle of incidence. We pointed out that incoherent Wood's anomaly is caused by the diffraction of the guided surface waves.

When the angle of incidence becomes close to one of the critical angles of incidence or close to a low grazing angle, error with respect to the optical theorem becomes large. This means that our iterative solution is not good enough for such angles of incidence. Therefore, practical methods of approximation must be studied to obtain a highly accurate solution.

Our discussion was limited to the single defect case in the periodic grating. However, there are other mathematical models of periodic grating with defects: one is a case with double or finite number of defects of which positions are known. Another model is a case with random defects, that is, the defect probability is known but their positions are unknown. It is theoretically interesting to study such periodic gratings with defects. Although it is practically important to consider a metallic or dielectric grating with single defect for the optical measurement or inspection, it is still difficult to treat the cases with defects for such materials. However, these problems are left for the future studies.

References

[1] P. Sheng, R.S. Stepleman, and P.N. Sanda, "Exact eigenfunctions for square-wave gratings: Application to diffraction and surface-plasmon calculations," Phys. Rev. B, vol.26, no.6, pp.2907–2917, 1982.

[2] J.A. Sanhez-Gil and A. Maradudin, "Dynamic near-field calculations of surface-plasmon polariton pulses resonantly scattered at sub-micron metal defects," Opt. Express, vol.12, no.5, pp.883–894, 2004.

[3] R. Sato and H. Shirai, "Electromagnetic plane wave scattering by a loaded trough on a ground plane," IEICE Trans. Electron., vol.E77-C, no.12, pp.1983–1989, Dec. 1994.

[4] R. Sato and H. Shirai, "Electromagnetic plane wave scattering by a gap on a ground plane," IEICE Trans. Electron. (Japanese Edition), vol.J80-C-I, no.5, pp.179–185, May 1997.

[5] R.A. Depine and D.C. Skigin, "Scattering from metallic surface having finite number of rectangular grooves," J. Opt. Soc. Am., vol.A11, no.11, pp.2844–2850, 1994.

[6] N. Bruce, "Control of the backscattered intensity in random rectangular-groove surfaces with variations in the groove depth," Appl. Opti., vol.44, no.5, pp.784–791, 2005.

[7] H. Sekiguchi and H. Shirai, "Electromagnetic scattering analysis for crack depth estimation," IEICE Trans. Electron., vol.E86-C, no.11, pp.2224–2229, Nov. 2003.

[8] K. Hattori and J. Nakayama, "Scattering of TE plane wave from periodic grating with single defect," IEICE Trans. Electron., vol.E90-C, no.2, pp.312–319, Feb. 2007.

[9] R. Petit, ed., Electromagnetic theory of gratings, Springer, Berlin, 1980.

[10] A.D. Arsenieva and A.A. Maradudin, "Scattering of light from random surfaces that are periodic on average," Opt. Lett., vol.18, no.19, pp.1588–1590, 1993.

[11] L. Gao and J. Nakayama, "Scattering of a TM plane wave from periodic random surfaces," Waves in Random Media, vol.9, pp.53–67, 1999.

[12] A. Hessel and A.A. Olinear, "A new theory of Wood's anomalies on optical gratings," Appl. Opt., vol.4, no.10, pp.1275–1297, 1965.
[13] R.W. Wood, "On a remarkable case of uneven distribution of light in a diffraction grating spectrum," Phil. Mag., vol.4, pp.396–402, 1902.
[14] C. Bohren and D. Huffman, Absorption and scattering of light by small particles, Wiley, New York, 1983.
[15] A. Ishimaru, Wave propagation and scattering in random media, IEEE Press, New York, 1997.
[16] J. Nakayama, K. Mizutani, and M. Tsuneoka, "Scattering of electromagnetic waves from a perfectly conductive slightly rough surface: Depolarization in backscatter," Math. Physics, vol.27, no.5, pp.1435–1448, 1986.
[17] Y. Tamura and J. Nakayama, "TM plane wave scattering and diffraction from a randomly rough half-plane: (part II) An evaluation of the diffraction kernel," Waves in Random and Complex Media, vol.16, pp.43–67, 2006.
[18] Y. Tamura and J. Nakayama, "Mass operator for wave scattering from a slightly random surface," Waves in Random Media, vol.9, pp.341–368, 1999.

Kazuhiro Hattori received the B.E. and M.E. degrees from Kyoto Institute of Technology in 1995 and 2000, respectively. From 2000 he works in the Research Laboratories, Mayekawa MFG, Ibaraki Pref. Currently, he is a graduate student at the Institute working toward Ph.D. degree.

Junichi Nakayama received the B.E. degree from Kyoto Institute of Technology in 1968, M.E. and Dr.Eng. degrees from Kyoto University in 1971 and 1982, respectively. From 1971 to 1975 he worked in the Radio Communication Division of Research Laboratories, Oki Electric Industry, Tokyo. In 1975, he joined the staff of Faculty of Engineering and Design, Kyoto Institute of Technology, where he is currently Professor of Electronics. From 1983 to 1984 he was a Visiting Research Associate in Department of Electrical Engineering, University of Toronto, Canada. Since 2002, he has been an Editorial Board member of *Waves in Random and Complex Media*. His research interests are electromagnetic wave theory, acoustical imaging and signal processing. Dr. Nakayama is a member of IEEE and a fellow of the Institute of Physics.

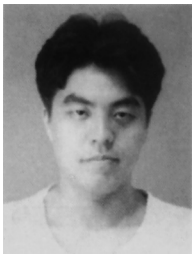

Yasuhiko Tamura received the B.E., M.E. and Ph.D. degrees from Kyoto Institute of Technology in 1991, 1993 and 2005, respectively. From 1993 to 1994 he worked in the Technical Research Institute, Konami Co., Ltd., Kobe. In 1994, he joined the staff of Faculty of Design and Engineering, Kyoto Institute of Technology. His research interests are electromagnetic wave theory, computational methods for stochastic analysis and visualization for electromagnetic field. Dr. Tamura received the Paper Presentation Award from Institute of Electrical Engineering of Japan in 1996.